Received: 8 March 2021 | Revised: 13 July 2021 | Accepted: 14 July 2021

DOI: 10.1111/epi.17019

Epilepsia®

FULL-LENGTH ORIGINAL RESEARCH

Two-trajectory laser amygdalohippocampotomy: Anatomic modeling and initial seizure outcomes

David D. Liu[1]* | Peter M. Lauro[1,2]* | Ronald K. Phillips III[1] | Owen P. Leary[1] | Bryan Zheng[1] | Julie L. Roth[3] | Andrew S. Blum[3] | David J. Segar[4] | Wael F. Asaad[1,2,5]

[1]Department of Neurosurgery, The Warren Alpert Medical School, Brown University, Providence, RI, USA

[2]Department of Neuroscience, Brown University, Providence, RI, USA

[3]Department of Neurology, The Warren Alpert Medical School, Brown University, Providence, RI, USA

[4]Department of Neurosurgery, Brigham and Women's Hospital, Harvard Medical School, Boston, MA, USA

[5]Norman Prince Neurosciences Institute, Rhode Island Hospital, Providence, RI, USA

Correspondence
David D. Liu, Department of Neurosurgery, The Warren Alpert Medical School, Brown University, Providence, RI 02903, USA.

Email: david_liu@brown.edu

Abstract

Objective: Laser interstitial thermal therapy (LITT) for mesial temporal lobe epilepsy (mTLE) is typically performed with one trajectory to target the medial temporal lobe (MTL). MTL structures such as piriform and entorhinal cortex are epileptogenic, but due to their relative geometry, they are difficult to target with one trajectory while simultaneously maintaining adequate ablation of the amygdala and hippocampus. We hypothesized that a two-trajectory approach could improve ablation of all relevant MTL structures. First, we created large-scale computer simulations to compare idealized one- vs two-trajectory approaches. A two-trajectory approach was then validated in an initial cohort of patients.

Methods: We used magnetic resonance imaging (MRI) from the Human Connectome Project (HCP) to create subject-specific target structures consisting of hippocampus, amygdala, and piriform/entorhinal/perirhinal cortex. An algorithm searched for safe potential trajectories along the hippocampal axis (catheter one) and along the amygdala-piriform axis (catheter two) and compared this to a single trajectory optimized over all structures. The proportion of each structure ablated at various burn radii was evaluated. A cohort of 11 consecutive patients with mTLE received two-trajectory LITT; demographic, operative, and outcome data were collected.

Results: The two-trajectory approach was superior to the one-trajectory approach at nearly all burn radii for all hippocampal subfields and amygdala nuclei ($p < .05$). Two-laser trajectories achieved full ablation of MTL cortical structures at physiologically realistic burn radii, whereas one-laser trajectories could not. Five patients with at least 1 year of follow-up (mean = 21.8 months) experienced Engel class I outcomes; 6 patients with less than 1 year of follow-up (mean = 6.6 months) are on track for Engel class I outcomes.

*David D. Liu and Peter M. Lauro contributed equally to this work.

Significance: Our anatomic analyses and initial clinical results suggest that LITT amygdalohippocampotomy performed via two-laser trajectories may promote excellent seizure outcomes. Future studies are required to validate the long-term clinical efficacy and safety of this approach.

KEYWORDS
computer simulation, entorhinal cortex, laser interstitial thermal therapy, medial temporal lobe epilepsy, piriform cortex

1 | INTRODUCTION

Epilepsy is the most prevalent chronic neurologic disorder, leading to considerable neurologic, cognitive, and psychosocial morbidity.[1, 2] Patients with drug-resistant mesial temporal lobe epilepsy (mTLE) may be offered surgical therapy. Although resection with anterior temporal lobectomy (ATL) remains the gold standard surgical therapy,[3] magnetic resonance imaging (MRI)–guided laser interstitial thermal therapy (LITT) is an increasingly popular, minimally invasive, stereotactic surgical therapeutic alternative with impressive outcomes in terms of seizure freedom,[4–8] reduced morbidity,[9] and improved neurocognitive function.[10–12]

Numerous studies have suggested that optimizing laser catheter trajectories to target epileptogenic anatomical structures, particularly the amygdala and mesial hippocampal head, may improve seizure-freedom rates.[4, 13] However, other mesial temporal lobe (MTL) structures have been implicated in epilepsy. For example, the role of the piriform cortex as a node in numerous cortical and subcortical olfactory networks has been theorized to contribute to the pathogenesis of mTLE,[14, 15] and clinical evidence suggests that increased resection of the piriform cortex is strongly associated with improved seizure-free outcomes.[16] However, due to the geometric orientation of the piriform cortex relative to amygdalohippocampal structures, satisfactory ablation is difficult to achieve in conventional single-laser trajectory LITT without reducing the ablation of other MTL structures. We therefore aimed to analyze the anatomy of MTL structures to formally compare one- vs two-trajectory approaches to laser ablation, especially with respect to achieving maximal ablation of MTL cortical areas without sacrificing ablation of critical amygdalohippocampal structures. Furthermore, we sought to review our initial experience with two-trajectory laser amygdalohippocampotomy, examining seizure and imaging outcomes using this surgical strategy.

Key Points

- Anatomic analysis shows that it is theoretically impossible to ablate all mesial temporal lobe (MTL) structures with a one-laser trajectory.
- Artificial intelligence algorithms find optimal two-laser trajectories along the axes of the hippocampus and amygdala/piriform cortex.
- Two-laser trajectories achieve greatly improved ablation volumes of critical MTL structures associated with seizure freedom.
- Clinical outcomes of two-trajectory laser interstitial thermal therapy (LITT) in a small cohort of five patients with more than 1-year of follow-up demonstrate Engel class Ia or Ib outcomes.
- The seizure and neuropsychological outcomes of two-trajectory LITT need to be confirmed in larger prospective studies.

In this article we describe a technique we developed to simulate LITT trajectories in high-quality Human Connectome Project (HCP) neuroimaging data sets and to optimize trajectories for targeting MTL structures using a computational search algorithm. These simulated anatomic results show that a two-trajectory approach for LITT amygdalohippocampotomy significantly improves ablation volumes of MTL structures relative to a one-laser approach, especially of the piriform and neighboring (entorhinal, perirhinal, parahippocampal) cortices. Early clinical and imaging outcomes of patients with mTLE who underwent two-trajectory LITT

demonstrate the feasibility and potential efficacy of this approach.

2 | METHODS

2.1 | HCP data

We used the U100 data set (54 female, 46 male, mean and SD 29.1 ± 3.7 years) within the WU-Minn HCP data set provided through the HCP public interface (http://db.humanconnectome.org/).[17,18] Each subject's T1-weighted MRI in Montreal Neurological Institute (MNI) common atlas space was downloaded, and subcortical and cortical structures were segmented using the FreeSurfer image analysis suite[19](version 7.0), by using the "recon-all" pipeline without skull-stripping. Additional FreeSurfer segmentation of hippocampal subfields and nuclei of the amygdala[20] was performed. Because FreeSurfer does not segment piriform cortex, the MNI coordinates of piriform cortex were extracted from the MNI Glasser atlas and overlaid onto the subject segmentation.[21] The Analysis of Functional NeuroImages (AFNI) and Surface Mapper (SUMA) software packages[22–24] were used to create subject-specific left-sided target surfaces corresponding to the regions of interest

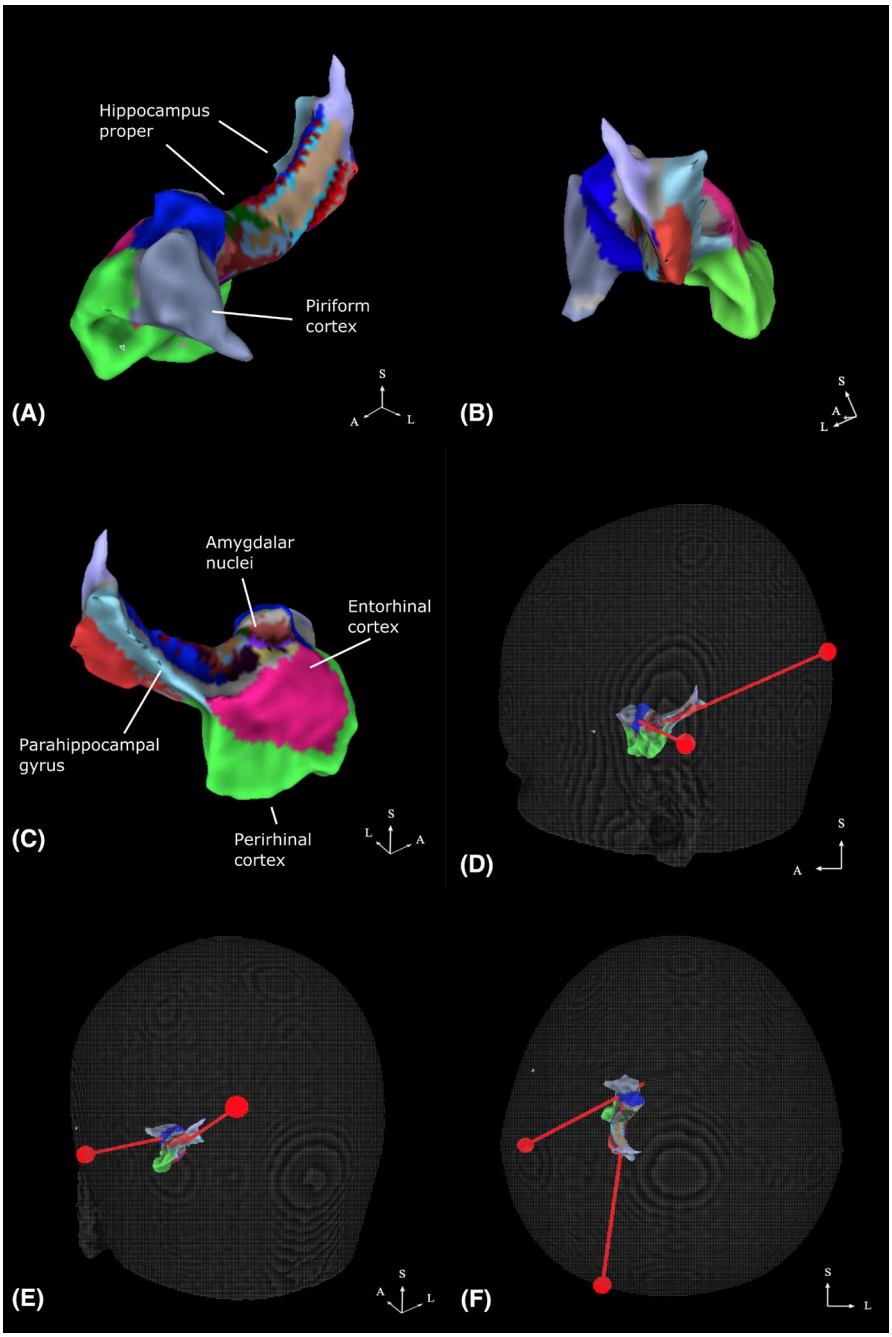

FIGURE 1 Mesial temporal lobe (MTL) structures and laser catheter entry points. Views of MTL structures (L = left, S = superior, A = anterior), looking medial-lateral (A), anterior-posterior (B), lateral-medial (C). Dark gray, piriform cortex; bright pink, entorhinal cortex; light blue, parahippocampal gyrus; bright green, perirhinal cortex. Other colors: hippocampal and amygdala subfields. (D-E) Laser catheter trajectories are shown in red on a reference head, with spheres indicating point of entry.

(ROIs) for this study: hippocampus, amygdala, piriform cortex, entorhinal cortex, perirhinal cortex, and parahippocampal gyrus (Figure 1A-C).

2.2 | Trajectory selection algorithm

The search space of trajectories was defined as all vectors spanning a "safe zone" of the skull for the entry point of the catheter and a "target volume" of MTL structures for the terminal point of the catheter. The safe zone excluded entry points that would violate the superior sagittal sinus, Sylvian fissure, or lateral ventricles. These structures were segmented manually on the MNI152 Atlas brain in 3DSlicer,[25] and any trajectories violating these structures were rejected. Entry points were constrained to be 1 cm lateral to the superior sagittal sinus and posterior to the posterosuperior insertion of the pinna, as trajectories anterior to this point were observed to pass through the Sylvian fissure.

For the one-trajectory case, the target volume was defined as all ROIs listed above. For the two-trajectory case, two target volumes were created: (1) a volume including all hippocampal, entorhinal, perirhinal, and parahippocampal ROIs (with the resulting trajectory defined as the hippocampal axis); and (2) a volume with amygdala and piriform cortex (with the resulting trajectory defined as the amygdala-piriform axis). We created a search algorithm for the trajectory that maximizes ablation by using the principal vector of each subject's target volume as a heuristic. For each subject, the space of possible trajectories was on the order of 10^{10}, arising from all pairwise voxel combinations from the safe zone to the target volume.

We constrained the search space by sampling trajectories based on their likelihood of being optimal. Intuitively, the volume intersected by a trajectory is proportional to its projection onto the volume's principal eigenvector. Thus we designated the point where the principal eigenvector intersects the skull as the "root point." For the amygdala-piriform target volume (targeted by the second laser trajectory), the principal eigenvector did not pass through the safe zone, so the root point was defined as the trajectory that maximized the projection onto the principal eigenvector. To further reduce the search space, the target volume was down-sampled so that no points were closer than two voxels together.

On each step of search, with probability 0.9, the safe zone was sampled for a point within a 20-voxel ball of the root point. Voxel volume was 1.0 mm^3. With probability 0.1, a random point on the safe zone was sampled instead. Sampling was performed without replacement. All trajectories between the sample point and the down-sampled target surface (on the order of 100 voxels) were drawn, and their ablation volumes with a hypothetical 10 mm burn radius were calculated. A total of 5000 iterations of this search procedure were repeated, and the trajectory with the maximum ablation volume was selected as the optimal trajectory. We note that after about 1000 iterations, the optimal trajectory and optimal volume ablated changed minimally, suggesting that the search space is globally convex, and thus the algorithm enjoys good convergence properties. This trajectory-search process was undertaken independently for each HCP subject. These simulations were performed on a Lambda Blade cluster (64-core, 256GB RAM; Lambda Labs Inc.) with a total runtime of 4 days.

2.3 | Optimal trajectory analysis

Once optimal trajectories were found in each subject, ablation volume was analyzed at gradually increasing radii ranging from 1 to 20 mm. Burn trajectory surfaces were generated in SUMA, and degree of overlap was quantified using the AFNI[23] 3dcalc program. Statistical significance of ablation volumes between one-laser and two-laser trajectories was evaluated using a two-sample t test with Benjamini-Hochberg correction for multiple comparisons with an adjusted q-value threshold of 0.05. For each structure, a receiver-operating characteristic (ROC) curve was traced out across all radii, by comparing ablation volumes of both placement plans, and area under the curve (AUC) was calculated for each ablated structure. The AUC ranges from $[-1, 1]$, with 0 representing equality.

2.4 | Patient population

All patients who underwent two-laser LITT for medically refractory mTLE between January 1, 2018 and December 31, 2020, at our institution were included in this analysis, irrespective of follow-up duration. There were no exclusion criteria based on availability of follow-up data. This study was approved by the institutional review board (IRB) as a retrospective chart review of the electronic medical record (EMR), which authorized exemption from informed consent requirements (local IRB #816619).

Demographic, intraoperative, and postoperative data were collected from all clinic and operative notes available for included subjects. Preoperative risk variables collected included MRI findings, scalp EEG, and long-term stereotactic encephalography (SEEG), when available. Postoperative outcome data included last available Engel and International League Against Epilepsy (ILAE) scale ratings.

Patient surgical lesions were identified by calculating the difference between preoperative T1-weighted and intraoperative gadolinium-enhanced T1-weighted volumes. Lesions were further refined by manually tracing out the

lesion cavity to ensure that lesion voxels were contained within the gadolinium ring enhancement (to prevent including hyperintense voxels corresponding to edema). To visualize the anatomic distribution of lesions across patients, each preoperative T1-weighted volume underwent a nonlinear transform to a standard MNI volume (MNI_2009c_T1).[26] This patient-specific transform was subsequently applied to each lesion and overlaid on a standard reference brain.

2.5 | Surgical technique

Patients were deemed candidates for stereotactic amygdalohippocampotomy at a multi-disciplinary conference (including neurologists, neuropsychologists, and neurosurgeons), after discussion of semiologic features, neuroimaging data, scalp EEG, and potentially other modalities, including SEEG data when available. A surgical plan was created using WayPoint Navigator planning software (FHC Inc.) planning software, with trajectories roughly concordant with the simulated optimal trajectories. A three-dimensional (3D)–printed stereotactic frame was created to assist with placement of the planned laser catheter trajectories (FHC Inc). Fiducial screws for the platform were placed in advance of trajectory planning. Once planning was complete and the platform received, the patient was brought to the operating room for placement of the cooling catheter/fiber optic laser assemblies (10 mm aperture catheters; Visualase System; Medtronic). Burr holes were created and bolts were placed in a standard fashion on the occipital-parietal scalp, including a posterior trajectory targeting the length of the hippocampus and a periauricular site targeting the amygdala and piriform cortex. Two separate cooling sheaths/fiber optic assemblies were placed, one for each trajectory.

The patient was then transported to the MRI scanner for ablation under imaging guidance using structural T1-sequence MRI as background with near–real-time MR thermography overlaid. In addition, a predicted lesion model using the Arrhenius equation on the time and temperature history of each voxel[27] was generated by the software and used in real time to help guide treatment. A single cooling circuit connected both sheaths in series, so that both were always cooled regardless of which laser was currently performing ablation, to prevent inadvertent cross-heating of these elements, particularly where the trajectories were in proximity (typically about 5–8 mm apart at the nearest point).

We first created an ablation along the hippocampal trajectory. We began the ablation anteriorly and stepwise retracted the fiberoptic catheter to ablate the length of the hippocampus and associated structures. Between three and five pull-back steps were used, with overlap varying from 2 to 5 mm per step. Low-temperature markers were placed on critical structures including the 3rd cranial nerve, midbrain, and optic radiations. Once we were satisfied with the hippocampal ablation, we turned our attention to the amygdala trajectory. The ablation was performed in a similar fashion, with typically one or two pull-back steps. After intraoperative MRI imaging was obtained to visually confirm adequate ablation (T1-weighted magnetization-prepared rapid acquisition with gradient echo (MPRAGE) with gadolinium contrast), all hardware was removed from the head.

3 | RESULTS

3.1 | Trajectory search characteristics

A total of 100 (one for each HCP subject) one-laser and two-laser placement plans were created according to the methods described above. The one-laser optimal trajectory was found to be generally consistent with the conventional entry point for LITT amygdalohippocampotomy, on the posterior surface of the skull, 1–2 cm lateral to the superior sagittal sinus, and at the level of the roof of the lateral ventricles. In the two-trajectory case, the laser targeting the hippocampus had an entry point comparable to that of the one-trajectory case, whereas the laser targeting the amygdala and piriform cortex had an entry point immediately superior to the superior-most extent of the helix (Figure 1D-F and Figure 2A,C,E). The aggregate patient lesions are shown in Figure 2B,D,F.

3.2 | Ablation of key MTL structures

The across-subject mean proportion of each MTL structure ablated at each radius is shown in Figure 3A-B. Most strikingly, at a maximum clinically viable ablation radius of 10 mm (the Visualase system supports radii between 2.5 and 10 mm[28]), the two-laser trajectory achieved 90% ablation of hippocampal head, hippocampal body, amygdala, and piriform. In contrast, the one-laser trajectory achieves only 90% ablation of the hippocampal body, whereas all other structures are less ablated, especially the piriform, perirhinal, and entorhinal cortices. The perirhinal and entorhinal cortices, likely due to their inferolateral location relative to amygdalohippocampal structures, are less than 50% ablated, even at clinically unviable radii of 15 and 18 mm, respectively. At lower ablation radii, the one-laser

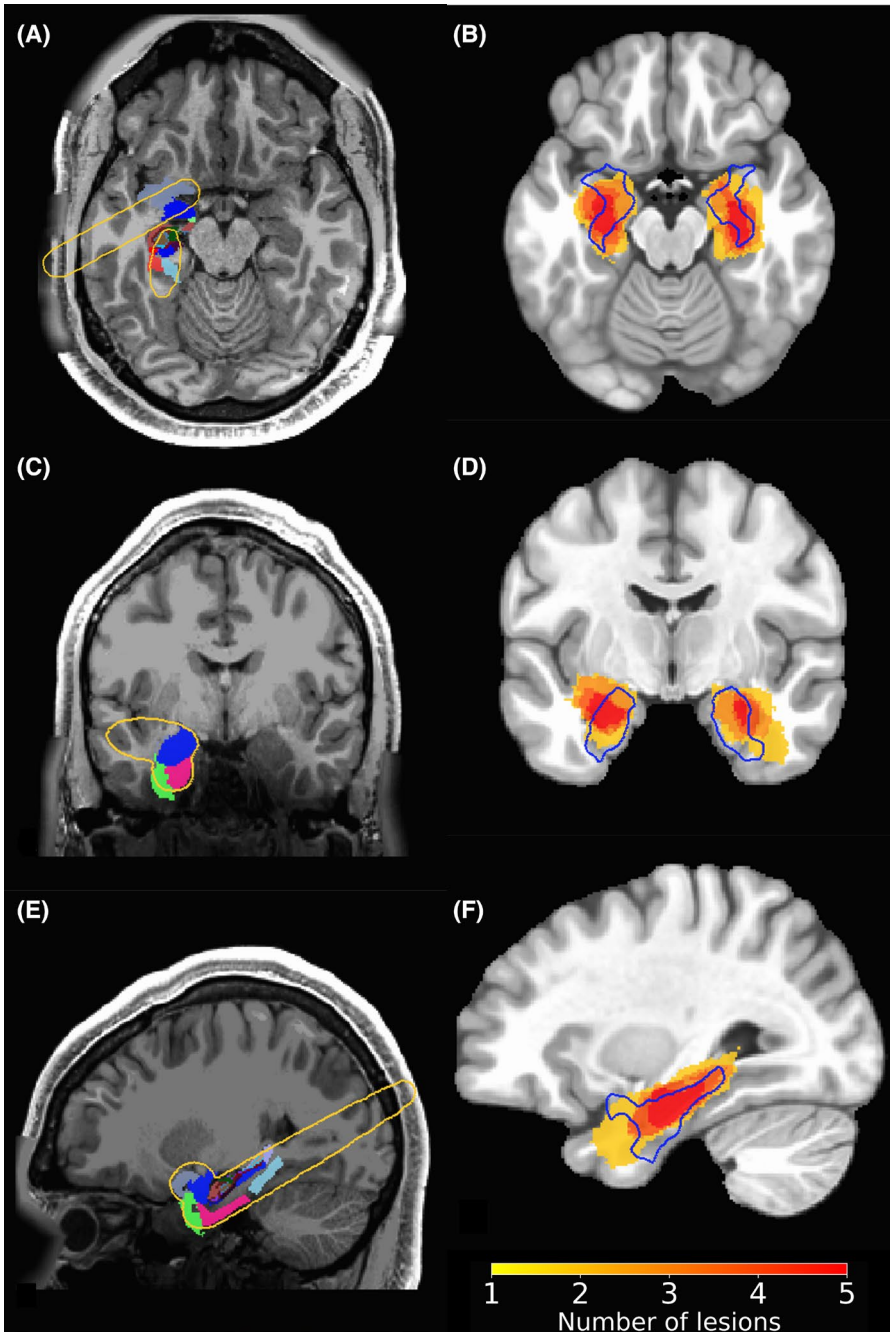

FIGURE 2 Simulated and real lesions. (A, C, E) Simulated two-laser trajectory with ablation radius of 7 mm, shown as orange outline. Dark gray in axial section (A), piriform cortex; bright green in sagittal section (E), perirhinal cortex; light blue and pink, parahippocampal gyrus. Other colors: hippocampal and amygdala subfields. (B, D, E) Patients' lesions mapped onto MNI atlas. Intensity of color represents the number of lesions at that location, and blue outline represents target structures.

trajectory has slightly improved ablation of hippocampal body and tail; however, these differences became statistically insignificant by a radius of 10 mm.

We have modeled ablation radii out to 20 mm, far beyond the clinically viable threshold of 10 mm, to demonstrate the theoretical anatomic implications and to fully trace out the ROC curves of these two approaches. The ROC curves (Figure 2C) yielded all positive AUCs, demonstrating the superiority of the two-laser trajectory for all structures, particularly entorhinal (AUC = 0.95) and perirhinal (AUC = 0.57) cortices. Ablation of the hippocampal body (AUC = 0.02) was most similar between the two trajectories.

3.3 | Ablation of hippocampal and amygdala subfields

The volume ablated of each subfield tended to follow the trend of its parent region for both the one-laser and two-laser cases. For example, the two-laser trajectory improved coverage of virtually all hippocampal head and amygdala subfields, at all radii (Table 1). This was particularly evident at smaller burn radii, where the amygdala ablation volumes differed by an order of magnitude. The hippocampal body was more equivocal. The two-laser trajectory improved coverage of most subfields of the hippocampus head proper (CA1, CA3)

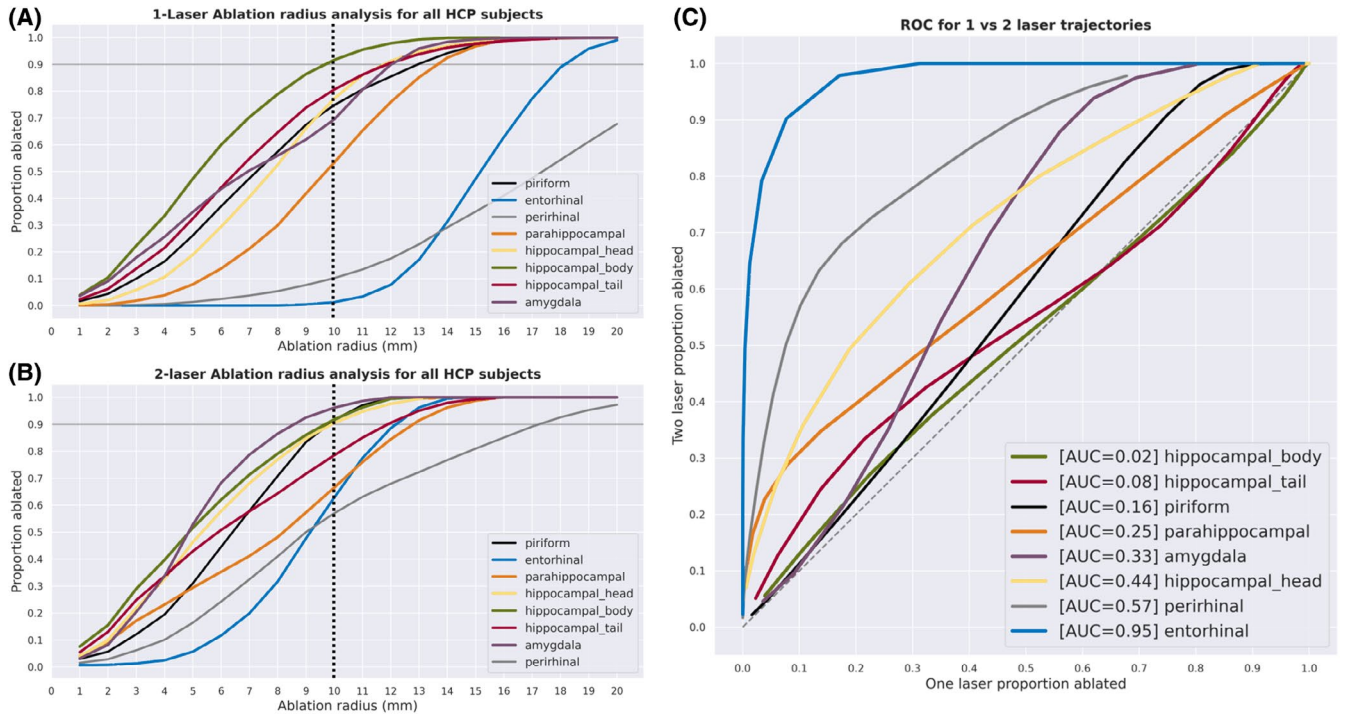

FIGURE 3 Ablation curves for one- and two-laser simulated trajectories. Satisfactory ablation threshold is defined as 0.9. (A) proportion of ROIs ablated by 1-laser trajectory; (B) proportion of ROIs ablated by two-laser trajectory; (C) receiver-operating characteristic (ROC) curve for one- vs two-laser trajectories. AUC ranges from −1 to 1, relative to the dashed line.

and related structures (presubiculum, subiculum, dentate gyrus). However, virtually all potential volumetric advantages of the one-laser trajectory disappeared by a radius of 12 mm.

3.4 | Patient characteristics and outcomes

Eleven patients (10F/1M, mean age = 35.9 ± 15.0) with medically refractory mTLE received two-laser LITT amygdalohippocampotomies. 9 of 11 (81%) of patients had evidence of mesial temporal sclerosis on MRI, 9 of 11 (81%) had concordant temporal lobe EEG and semiology, and of the two patients who underwent long-term SEEG monitoring, both had electrophysiologic evidence of MTL seizure activity with concordant lateralization.

One patient experienced a small catheter tract hemorrhage with mild right upper extremity drift that fully resolved on postoperative day 2. There were no other intraoperative or postoperative complications, including major hemorrhage, infection, or neurologic deficits. Two patients received two-trajectory LITT after initial treatment failure with one-trajectory LITT. An example intraoperative trajectory-aligned view is shown in Figure 4. At a median follow-up of 8 months, all patients experienced an improvement in seizure frequency and severity, relative to a baseline of medically refractory seizures (Table 2). Of the five patients who had more than 1-year of follow-up, all achieved Engel class I outcomes, three of whom experienced 1a seizure freedom. Of the six patients with less than 1-year of follow-up, Engel scores are not available, but all are projected to achieve Engel class I outcomes if their current clinical status is maintained.

4 | DISCUSSION

4.1 | Theoretical benefits of a two-laser trajectory

Although MRI-guided LITT amygdalohippocampotomy has emerged as a safe and effective treatment for mTLE, improved understanding of the anatomic constraints within this region will allow optimization of LITT trajectories. A large multi-center study suggested that increased ablation of the amygdala, hippocampal head, parahippocampal gyrus, and rhinal cortices was associated with better outcomes.[29] Geometrically, this corresponds to the entire axis of the hippocampus and amygdala, which can be achieved with one laser only given an appropriately large burn radius. However, the piriform cortex is an ellipsoid-shaped structure located anterolateral to the amygdala, and thus any trajectory oriented along the axis of the hippocampus

TABLE 1 Ablation statistics at various radii

	r = 3		r = 6		r = 9		r = 12	
Structure	**1L**	**2L**	**1L**	**2L**	**1L**	**2L**	**1L**	**2L**
Piriform cortex	0.100	0.105	0.370	**0.429**	0.675	**0.817**	0.855	**0.981**
Amygdala								
Lateral nucleus	0.000	0.003	0.000	**0.054**	0.003	**0.883**	0.344	**0.986**
Basal nucleus	0.000	**0.032**	0.008	**0.374**	0.080	**0.887**	0.665	**0.989**
Central nucleus	0.008	**0.094**	0.027	**0.599**	0.073	**0.950**	0.780	**0.992**
Medial nucleus	0.013	**0.104**	0.034	**0.602**	0.231	**0.932**	0.890	**0.998**
Cortical nucleus	0.010	**0.066**	0.054	**0.436**	0.271	**0.811**	0.803	**0.979**
Accessory basal nucleus	0.034	0.056	0.173	0.215	0.458	**0.632**	0.858	**0.975**
Corticoamygdaloid transition	0.099	0.109	0.256	**0.387**	0.477	**0.690**	0.855	**0.929**
Anterior amygdaloid area	0.107	0.098	0.308	0.377	0.547	0.663	0.845	**0.935**
Paralaminar nucleus	**0.152**	0.094	**0.454**	0.345	0.679	0.732	0.889	**0.944**
Entorhinal cortex	0.000	**0.007**	0.000	**0.114**	0.004	**0.477**	0.077	**0.881**
Perirhinal/ectorhinal cortex	0.002	**0.069**	0.024	**0.250**	0.076	**0.508**	0.175	**0.682**
Hippocampal head								
Parasubiculum	0.000	0.000	0.000	**0.227**	0.053	**0.730**	0.502	**0.956**
Presubiculum head	0.000	**0.252**	0.054	**0.932**	0.461	**0.995**	0.945	**1.000**
Subiculum head	0.000	**0.123**	0.019	**0.696**	0.411	**0.963**	0.959	**1.000**
CA1 head	0.051	**0.169**	0.273	**0.407**	0.614	**0.718**	0.866	**0.949**
CA3 head	0.327	0.327	**0.820**	0.764	0.981	0.959	0.999	1.000
CA4 head	0.050	**0.336**	0.641	**0.753**	0.972	**0.993**	0.998	1.000
Dentate head	0.057	**0.267**	0.432	**0.652**	0.887	**0.953**	0.988	**0.999**
Molecular layer head	0.063	**0.312**	0.293	**0.653**	0.791	**0.903**	0.970	**0.997**
Hippocampal body								
HATA	0.001	0.001	**0.088**	0.032	0.396	0.402	0.737	**0.834**
Presubiculum body	0.180	**0.463**	0.674	**0.828**	0.938	**0.972**	0.994	0.996
Subiculum body	0.204	**0.230**	0.636	0.662	0.948	0.955	0.999	1.000
CA1 body	0.005	0.001	0.053	0.042	0.296	0.321	**0.810**	0.677
CA3 body	**0.113**	0.035	**0.484**	0.355	**0.844**	0.729	0.996	0.991
CA4 body	**0.270**	0.175	**0.758**	0.635	0.987	0.971	1.000	1.000
Dentate body	0.362	0.338	**0.706**	0.632	0.946	0.904	1.000	1.000
Molecular layer body	0.231	**0.286**	**0.544**	0.504	**0.841**	0.770	0.992	0.985
Hippocampal tail	0.142	0.151	**0.468**	0.332	**0.738**	0.554	**0.895**	0.830
Parahippocampal gyrus								
Anterior parahippocampal	0.028	**0.173**	0.199	**0.361**	0.530	**0.622**	0.843	**0.910**
Posterior parahippocampal	0.001	**0.173**	0.034	**0.347**	0.228	**0.496**	0.617	**0.736**

Note: Bold values denote statistically significant Benjamini-Hochberg corrected *p*-values (<0.05) from Mann-Whitney tests comparing ablation volume between one-and two-laser trajectories.

Abbreviations: 1L, 1-laser; 2L, 2-laser; HATA, hippocampal–amygdalar transition area; r, radius.

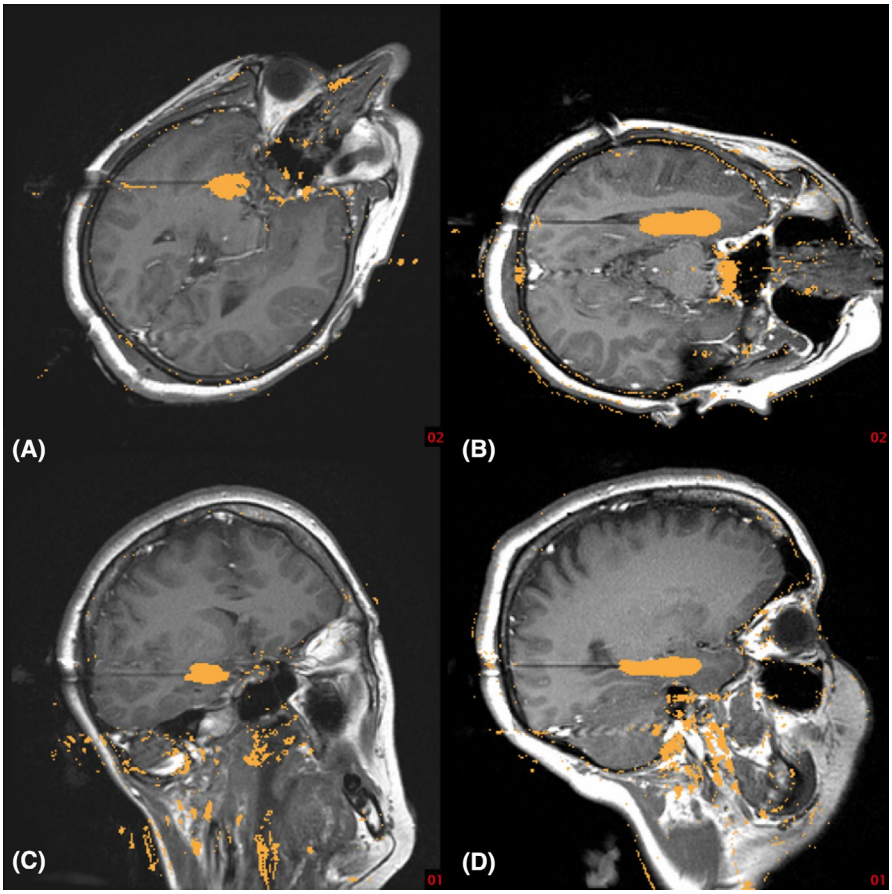

FIGURE 4 Procedural view of two-laser trajectory lesion estimates. (A, C) Trajectory-aligned T1 MRI imaging of amygdala-piriform laser. (B, D) Trajectory-aligned T1 MRI imaging of hippocampal laser.

and amygdala must trade off ablation of the amygdala with ablation of the piriform cortex (Figure 1). Similarly, the entorhinal and perirhinal cortices are located inferolateral to the hippocampus proper, and a hippocampal trajectory must trade off ablation of the amygdala and piriform cortex with ablation of these MTL cortices. A recent study also suggests that increased ablation of the parahippocampal gyrus improved seizure freedom, more than amygdalohippocampal structures.[30] Thus deviations in trajectory to account for any one structure may change the ablation efficacy of neighboring MTL structures, and thereby potentially reduce overall seizure reduction efficacy.

These considerations suggest that outcomes for mTLE with LITT can be improved by optimizing trajectory–volume ablation, constrained by anatomy such as the superior sagittal sinus, lateral ventricles, and Sylvian fissure. Prior computerized trajectory planning methods worked within these constraints to maximize ablation of the amygdalohippocampal complex,[13, 28] and these trajectories were validated in a multicenter cohort of 95 patients.[31] Another approach utilized machine learning to examine 7600 trajectories and their effects on amygdala, hippocampus, and parahippocampal gyrus.[32] However, the planning methods were limited to the use of one-laser trajectories. Although incremental progress in constrained optimization can reach a local maximum, introducing new approaches that fundamentally change the problem can reveal undiscovered global maxima.

Thus we considered how LITT amygdalohippocampotomy performed with two-laser trajectories instead of one-laser trajectories could change the angle of the LITT volume optimization problem. The benefits of this are twofold: improved ablation of the piriform cortex by utilizing the amygdala-piriform axis, and improved ablation of the hippocampal-amygdala axis and its parallel cortical structures by using dedicated lasers for each. Our algorithm searched through more than 100 million trajectories to select the top 100 trajectories for three different axes. Subsequent analyses suggest that these trajectories can achieve results that are theoretically impossible in the one-laser case. Notably, LITT is also utilized in neurosurgery for other pathologies, such as tumors[33] or intractable psychiatric disease,[34] which may also benefit from a similar optimization approach using more than one trajectory.

4.2 | Quantitative benefits of a two-laser trajectory

Our anatomic simulations demonstrated that two-trajectory LITT improved ablation of epileptogenic MTL structures such as the hippocampal head, amygdala, and

TABLE 2 Patient outcomes from two-laser LITT amygdalohippocampotomy

Age	Sex	Notes	Laterality	Power	Post-op Engel	Post-op ILAE	Length of follow-up	Complications
46	F	Two-laser, after one-laser 9 months prior (consistent seizures). After second procedure, rare simple partial seizures after months of seizure freedom.	Right	N/A	Ib	Class 3	26 months	None
41	F		Left	35%–50%	Ia	Class 1	25 months	Minor catheter tract hemorrhage; resolved.
39	F	One-laser, after one-laser 9 months prior (consistent seizures). Seizure-free after second procedure.	Right	60%–65%	Ia	Class 1	24 months	None
32	M		Left	50%–60%	Ia	Class 1	18 months	None
51	F	Rare nondisabling simple partial seizures.	Left	50%–80%	Ib	Class 2	16 months	None
54	F	Isolated case of generalized convulsions after self-discontinuing seizure medications.	Right	50%–70%	N/A	N/A	8 months	None
39	F	Seizure-free.	Left	60%–65%	N/A	N/A	8 months	None
6	F	Occasional auras.	Right	40%–75%	N/A	N/A	7 months	None
36	F	Seizure-free.	Right	50%–80%	N/A	N/A	7 months	None
28	F	Recurrent, but milder seizures since surgery. History of cerebral palsy.	Right	50%–70%	N/A	N/A	4 months	None

Note: Engel outcomes are only calculated for patients with follow-up greater than 1 year.

cortical structures. This result was most evident at clinically relevant ablation radii less than 10 mm; 10 mm is the maximum ablation radius supported by the widely used Visualase system.[28] For example, by 10 mm, two-trajectory LITT achieved 90% ablation of hippocampal head, hippocampal body, amygdala, and piriform cortex, whereas one-trajectory LITT required 13 mm to achieve 90% ablation of these structures (Figure 3). These results are also true for subfields of the hippocampus and nuclei of the amygdala (Table 1). An AUC analysis showed that the two-laser approach provided a relative advantage over the one-laser approach in all structures; however, this advantage was narrower in hippocampal body and tail. This may be because the one-laser approach was optimized along the long axis of the hippocampus. However, studies have suggested that hippocampal body and tail are the least important structures in terms of postoperative seizure freedom.[29]

In addition, one-trajectory LITT did not achieve satisfactory ablation of entorhinal or perirhinal cortices at viable burn radii. This is clear by examining the inferolateral position of these structures relative to the hippocampus and amygdala (Figure 1). Two-laser trajectories increase the geometric degrees of the freedom a surgeon can use to target various structures, which allows for better targeting of the piriform and rhinal cortices. For example, at a burn radius of 9 mm, the one-laser approach achieved only 0.005 and 0.0081 proportion ablation of entorhinal and perirhinal cortex, respectively, compared to about 0.5 for both structures for the two-laser approach. Further studies should determine the optimal radius size for two-trajectory LITT that can maximize ablation while minimizing damage to neighboring structures.

Our early clinical experience in a cohort of 11 patients suggests that the two-laser approach is safe. Only one patient experienced a mild operative complication, which resolved spontaneously, and this relatively low complication rate is consistent with the literature.[35] All patients with more than 1-year of follow-up achieved Engel class I outcomes, with three of these patients (60%) seizure-free and two (40%) with dramatic seizure reduction but occasional, nondisabling focal seizures

without loss of awareness. The six patients with less than 1-year of follow-up have also experienced seizure freedom or rare mild seizures, although Engel outcomes are not yet available. We note that the selection criteria for our cohort were not particularly strict (see Section 3), consistent with typical clinical criteria applied for determining LITT candidacy. These results are comparable to historical cohorts of one-trajectory LITT experience Engel class 1a seizure outcomes between 53% and 61%,[5, 8, 10, 36] although due to the small power of our clinical results, direct comparisons are not statistically rigorous, and we do not make any claims about the clinical superiority of two-trajectory LITT; rather, our clinical results demonstrate that this approach is feasible. Due to our short follow-up and small cohort, the ability to draw definitive clinical conclusions is limited. Although the anatomic analysis provides a strong theoretical basis for the potential success of the two-laser approach, larger cohorts with long-term follow-up are needed for validation.

4.3 | Improved coverage of piriform cortex

Targeting of the piriform cortex is justified by increasing basic science and clinical studies demonstrating its involvement in the pathogenesis of mTLE. The piriform cortex, particularly the endopiriform nucleus,[37] is involved in numerous olfactory networks, anecdotally associated with the olfactory auras associated with some seizures.[14] A study in rodents demonstrated that miniscule injections of cholinergic agents to piriform cortex generated bilateral clonic seizures, an effect that was not replicated in other MTL structures.[38] Conversely, a recent study showed that electrical stimulation of the endopiriform nucleus improved seizure outcomes in mice.[39] In humans, a multicenter 2019 study of 107 adults demonstrated that removal of at least half of the piriform cortex in ATL increased the odds of seizure freedom by 16-fold, and that these odds were directly proportional to the extent of piriform resection.[16] These studies suggest that increased ablation of piriform cortex would also be associated with improved outcomes. To our knowledge, no studies have studied the optimization of piriform cortex ablation in LITT.

4.4 | Improved coverage of entorhinal and perirhinal cortices

There is increasing basic science evidence that the entorhinal cortex is associated with epileptic seizures. The entorhinal cortex, as a node in the circuit of Papez, contributes to the cortical and subcortical networks,[37] and its role in seizure genesis and propagation has been shown in recent optogenetic animal models.[40, 41] Perirhinal cortex has also been associated with limbic mTLE seizures,[42] although the scientific evidence for entorhinal cortex is stronger. In addition, imaging studies have shown that the volume of the rhinal cortices are decreased in patients with mTLE.[43, 44] However, a recent study in a cohort of 18 patients who underwent stereotactic mTLE ablation showed that there was no statistically significant correlation between volume reduction in entorhinal and perirhinal cortex and Engel class I outcomes,[45] prompting further investigation of the clinical importance of perirhinal and entorhinal ablation. Due to the patient-specific heterogeneity of epileptogenic circuits,[46] it is feasible that entorhinal and perirhinal ablation would preferentially benefit some patients but not others.

4.5 | Limitations

Although our simulated trajectories offer an anatomic basis for two-trajectory LITT, they were calculated in healthy controls, who had potentially different structural volumes and morphology, and who did not receive angiography to account for smaller vessels or ependymal surfaces. We note that if these trajectories were to be used in a clinical setting, they could be adjusted to be surgically feasible and incorporated into existing planning software. In addition, patients with mTLE often have hippocampal sclerosis, which is associated with atrophy of the MTL structures on imaging[47, 48]; this could exaggerate ablation volumes. This does not change the broader geometry or orientation of MTL structures, which form the basis of our analysis, but may change the relative sizes and positions of MTL structures, which could allow for better targeting of basal structures.

Longer-term follow-up and a larger patient sample are necessary to validate the clinical outcomes of this technique and to perform large-scale anatomic analyses of patient lesions. Future studies will quantify ablation of patient structures and subfields. A prospectively designed trial with one and two trajectory groups would be required to directly compare the clinical efficacy of the two approaches. Finally, the lack of neuropsychologic outcomes to assess whether the two-trajectory approach continues to spare significant cognitive and memory function, as has been reported for the standard one-trajectory approach, is a major limitation.[10–12] Such data are now being collected prospectively.

5 | CONCLUSION

Our results suggest that two-trajectory LITT amygdalohippocampotomy improved ablation of hippocampus, amygdala, and neighboring cortical structures, especially piriform cortex. An anatomic simulation on healthy control imaging demonstrated the theoretical grounds for using one laser to target the hippocampal-amygdala axis and another laser to target the amygdala-piriform axis, and a small clinical cohort demonstrated the safety and early efficacy of this technique. If confirmed through prospective validation, this technique will have practical implications for neurosurgeons who offer LITT ablation for mTLE.

ACKNOWLEDGEMENTS

We are grateful for the generous participation of our patients in this study, and for the care provided by the physicians and staff at Rhode Island Hospital. We also thank Kelsea Laubenstein-Parker for technical assistance, Karina Bertsch for administrative support, and Ann Duggan-Winkle for clinical support. This work was supported by an NIH Training Grant (NINDS T32MH020068) to P.M.L., a Doris Duke Clinical Scientist Development Award (#2014101) to W.F.A., an NIH COBRE Award: NIGMS P20 GM103645 (PI: Jerome Sanes) supporting W.F.A., a Neurosurgery Research and Education Foundation (NREF) grant to W.F.A., the Lifespan Norman Prince Neurosciences Institute, and the Brown University Robert J. and Nancy D. Carney Institute for Brain Science. Part of this research was conducted using computational resources and services at the Center for Computation and Visualization at Brown University, with funding provided by an NIH Office of the Director grant S10OD025181.

CONFLICT OF INTEREST

None of the authors has any conflict of interest to disclose. We confirm that we have read the Journal's position on issues involved in ethical publication and affirm that this report is consistent with those guidelines.

AUTHOR CONTRIBUTIONS

Conceptualization: WFA, PML, DDL, DJS. Data: PML, DDL, RKP, OPL, BZ. Software: PML, DDL. Analyses: DDL, PML. Manuscript writing: DDL, PML, WFA. All authors reviewed and edited the manuscript.

ORCID

David D. Liu https://orcid.org/0000-0003-2313-1890
Peter M. Lauro https://orcid.org/0000-0002-8569-6427
Owen P. Leary https://orcid.org/0000-0002-6282-828X
Wael F. Asaad https://orcid.org/0000-0003-4406-9096

REFERENCES

1. Fisher RS, van Emde BW, Blume W, Elger C, Genton P, Lee P, et al. Epileptic seizures and epilepsy: definitions proposed by the International League Against Epilepsy (ILAE) and the International Bureau for Epilepsy (IBE). Epilepsia. 2005;46:470–2.
2. Thurman DJ, Beghi E, Begley CE, Berg AT, Buchhalter JR, Ding D, et al. Standards for epidemiologic studies and surveillance of epilepsy. Epilepsia. 2011;52(Suppl 7):2–26.
3. Wiebe S, Blume WT, Girvin JP, Eliasziw M. A randomized, controlled trial of surgery for temporal-lobe epilepsy. N Engl J Med. 2001;345:311–8.
4. Jermakowicz WJ, Kanner AM, Sur S, Bermudez C, D'Haese PF, Kolcun JPG, et al. Laser thermal ablation for mesiotemporal epilepsy: analysis of ablation volumes and trajectories. Epilepsia. 2017;58:801–10.
5. Kang JY, Wu C, Tracy J, Lorenzo M, Evans J, Nei M, et al. Laser interstitial thermal therapy for medically intractable mesial temporal lobe epilepsy. Epilepsia. 2016;57:325–34.
6. Tao JX, Wu S, Lacy M, Rose S, Issa NP, Yang CW, et al. Stereotactic EEG-guided laser interstitial thermal therapy for mesial temporal lobe epilepsy. J Neurol Neurosurg Psychiatry. 2018;89:542–8.
7. Grewal SS, Zimmerman RS, Worrell G, Brinkmann BH, Tatum WO, Crepeau AZ, et al. Laser ablation for mesial temporal epilepsy: a multi-site, single institutional series. J Neurosurg. 2018;1–8.
8. Le S, Ho AL, Fisher RS, Miller KJ, Henderson JM, Grant GA, et al. Laser interstitial thermal therapy (LITT): seizure outcomes for refractory mesial temporal lobe epilepsy. Epilepsy Behav. 2018;89:37–41.
9. Willie JT, Laxpati NG, Drane DL, Gowda A, Appin C, Hao C, et al. Real-time magnetic resonance-guided stereotactic laser amygdalohippocampotomy for mesial temporal lobe epilepsy. Neurosurgery. 2014;74:569–84.
10. Gross RE, Stern MA, Willie JT, Fasano RE, Saindane AM, Soares BP, et al. Stereotactic laser amygdalohippocampotomy for mesial temporal lobe epilepsy. Ann Neurol. 2018;83:575–87.
11. Drane DL, Loring DW, Voets NL, Price M, Ojemann JG, Willie JT, et al. Better object recognition and naming outcome with MRI-guided stereotactic laser amygdalohippocampotomy for temporal lobe epilepsy. Epilepsia. 2015;56:101–13.
12. Donos C, Breier J, Friedman E, Rollo P, Johnson J, Moss L, et al. Laser ablation for mesial temporal lobe epilepsy: surgical and cognitive outcomes with and without mesial temporal sclerosis. Epilepsia. 2018;59:1421–32.
13. Wu C, Boorman DW, Gorniak RJ, Farrell CJ, Evans JJ, Sharan AD. The effects of anatomic variations on stereotactic laser amygdalohippocampectomy and a proposed protocol for trajectory planning. Neurosurgery. 2015;11(Suppl 2):345–56.
14. Vaughan DN, Jackson GD. The piriform cortex and human focal epilepsy. Front Neurol. 2014;5:259.
15. Curia G, Lucchi C, Vinet J, Gualtieri F, Marinelli C, Torsello A, et al. Pathophysiogenesis of mesial temporal lobe epilepsy: is prevention of damage antiepileptogenic? Curr Med Chem. 2014;21:663–88.
16. Galovic M, Baudracco I, Wright-Goff E, Pillajo G, Nachev P, Wandschneider B, et al. Association of piriform cortex resection

with surgical outcomes in patients with temporal lobe epilepsy. JAMA Neurol. 2019;76:690–700.
17. Van Essen DC, Smith SM, Barch DM, Behrens TE, Yacoub E, Ugurbil K, et al. The WU-Minn human connectome project: an overview. NeuroImage. 2013;80:62–79.
18. Marcus DS, Harwell J, Olsen T, Hodge M, Glasser MF, Prior F, et al. Informatics and data mining tools and strategies for the human connectome project. Front Neuroinform. 2011;5:4.
19. Fischl B. FreeSurfer. Neuroimage. 2012;62:774–81.
20. Iglesias JE, Augustinack JC, Nguyen K, Player CM, Player A, Wright M, et al. A computational atlas of the hippocampal formation using ex vivo, ultra-high resolution MRI: application to adaptive segmentation of in vivo MRI. NeuroImage. 2015;115:117–37.
21. Glasser MF, Coalson TS, Robinson EC, Hacker CD, Harwell J, Yacoub E, et al. A multi-modal parcellation of human cerebral cortex. Nature. 2016;536:171–8.
22. Argall BD, Saad ZS, Beauchamp MS. Simplified intersubject averaging on the cortical surface using SUMA. Hum Brain Mapp. 2006;27:14–27.
23. Cox RW. AFNI: software for analysis and visualization of functional magnetic resonance neuroimages. Comput Biomed Res. 1996;29:162–73.
24. Saad ZS, Reynolds RC. SUMA. Neuroimage. 2012;62:768–73.
25. Kikinis R, Pieper SD, Vosburgh KG. 3D slicer: A platform for subject-specific image analysis, visualization, and clinical support. In: Jolesz FA, editor. Intraoperative Imaging and Image-Guided Therapy. New York, NY: Springer; 2014. p. 277–89.
26. Fonov VS, Evans AC, McKinstry RC, Almli CR, Collins DL. Unbiased nonlinear average age-appropriate brain templates from birth to adulthood. NeuroImage. 2009;47:S102.
27. Fasano A, Hömberg D, Naumov D. On a mathematical model for laser-induced thermotherapy. Appl Math Model. 2010;34:3831–40.
28. Vakharia VN, Sparks R, Li K, O'Keeffe AG, Miserocchi A, McEvoy AW, et al. Automated trajectory planning for laser interstitial thermal therapy in mesial temporal lobe epilepsy. Epilepsia. 2018;59:814–24.
29. Wu C, Jermakowicz WJ, Chakravorti S, Cajigas I, Sharan AD, Jagid JR, et al. Effects of surgical targeting in laser interstitial thermal therapy for mesial temporal lobe epilepsy: a multicenter study of 234 patients. Epilepsia. 2019;60:1171–83.
30. Satzer D, Tao JX, Warnke PC. Extent of parahippocampal ablation is associated with seizure freedom after laser amygdalohippocampotomy. J Neurosurg. 2021;aop:1–10.
31. Vakharia VN, Sparks RE, Li K, O'Keeffe AG, Pérez-García F, França LGS, et al. Multicenter validation of automated trajectories for selective laser amygdalohippocampectomy. Epilepsia. 2019;60:1949–59.
32. Li K, Vakharia VN, Sparks R, França LGS, Granados A, McEvoy AW, et al. Optimizing trajectories for cranial laser interstitial thermal therapy using computer-assisted planning: a machine learning approach. Neurotherapeutics. 2019;16:182–91.
33. O'Connor KP, Palejwala AH, Milton CK, Lu VM, Glenn CA, Sughrue ME, et al. Laser interstitial thermal therapy case series: choosing the correct number of fibers depending on lesion size. Oper Neurosurg. 2020;20:18–23.
34. Lauro PM, Lee S, Ahn M, Barborica A, Asaad WF. DBStar: an open-source tool kit for imaging analysis with patient-customized deep brain stimulation platforms. Stereotact Funct Neurosurg. 2018;96:13–21.
35. Wicks RT, Jermakowicz WJ, Jagid JR, Couture DE, Willie JT, Laxton AW, et al. Laser interstitial thermal therapy for mesial temporal lobe epilepsy. Neurosurgery. 2016;79:S83–91.
36. Cajigas I, Kanner AM, Ribot R, Casabella AM, Mahavadi A, Jermakowicz W, et al. Magnetic resonance-guided laser interstitial thermal therapy for mesial temporal epilepsy: a case series analysis of outcomes and complications at 2-year follow-up. World Neurosurg. 2019;126:e1121–9.
37. Vismer MS, Forcelli PA, Skopin MD, Gale K, Koubeissi MZ. The piriform, perirhinal, and entorhinal cortex in seizure generation. Front Neural Circuits. 2015;9:27.
38. Piredda S, Gale K. A crucial epileptogenic site in the deep prepiriform cortex. Nature. 1985;317:623–5.
39. Li D, Luo D, Wang J, Wang W, Yuan Z, Xing Y, et al. Electrical stimulation of the endopiriform nucleus attenuates epilepsy in rats by network modulation. Ann Clin Transl Neurol. 2020;7:2356–69.
40. Janz P, Savanthrapadian S, Häussler U, Kilias A, Nestel S, Kretz O, et al. Synaptic remodeling of entorhinal input contributes to an aberrant hippocampal network in temporal lobe epilepsy. Cereb Cortex. 2016;27:2348–64.
41. Lu Y, Zhong C, Wang L, Wei P, He W, Huang K, et al. Optogenetic dissection of ictal propagation in the hippocampal–entorhinal cortex structures. Nat Commun. 2016;7:e10962.
42. Kelly ME, McIntyre DC. Perirhinal cortex involvement in limbic kindled seizures. Epilepsy Res. 1996;26:233–43.
43. Bernasconi N, Bernasconi A, Caramanos Z, Antel SB, Andermann F, Arnold DL. Mesial temporal damage in temporal lobe epilepsy: a volumetric MRI study of the hippocampus, amygdala and parahippocampal region. Brain. 2003;126:462–9.
44. Bernasconi N, Bernasconi A, Andermann F, Dubeau F, Feindel W, Reutens DC. Entorhinal cortex in temporal lobe epilepsy: a quantitative MRI study. Neurology. 1999;52:1870.
45. Malikova H, Liscak R, Vojtech Z, Prochazka T, Vymazal J, Vladyka V, et al. Stereotactic radiofrequency amygdalohippocampectomy: does reduction of entorhinal and perirhinal cortices influence good clinical seizure outcome? Epilepsia. 2011;52:932–40.
46. Jooma R, Yeh HS, Privitera MD, Rigrish D, Gartner M. Seizure control and extent of mesial temporal resection. Acta Neurochir. 1995;133:44–9.
47. Chan S, Erickson JK, Yoon SS. Limbic system abnormalities associated with mesial temporal sclerosis: a model of chronic cerebral changes due to seizures. Radiographics. 1997;17:1095–110.
48. Coan AC, Kubota B, Bergo FPG, Campos BM, Cendes F. 3T MRI quantification of hippocampal volume and signal in mesial temporal lobe epilepsy improves detection of hippocampal sclerosis. Am J Neuroradiol. 2014;35:77–83.

How to cite this article: Liu DD, Lauro PM, Phillips RK III, Leary OP, Zheng B, Roth JL, et al. Two-trajectory laser amygdalohippocampotomy: Anatomic modeling and initial seizure outcomes. Epilepsia. 2021;00:1–13. https://doi.org/10.1111/epi.17019